Desalination and Water Treatment
www.deswater.com

doi: 10.5004/dwt.2018.21081

113 (2018) 88–101
May

Simultaneous adsorption of Cr(VI) ions and phenol onto commercial granular activated carbon NORIT 1240: Artificial neural network modeling and central composite design optimization

Dorra Tabassi*, Soumaya Harbi, Bechir Hamrouni

Desalination and Water Treatment Research Unit (UR11ES17), Faculty of Science of Tunis, University of Tunis El Manar, 2092 Manar I, Tunisia Tel./Fax + 216 71 871 282, email: dorratabassi@gmail.com

Received 16 January 2016; Accepted 1 March 2018

ABSTRACT

Simultaneous adsorption of Cr(VI) ions and phenol, which are frequently encountered together in wastewaters, onto granular activated carbon (GAC) was investigated. The adsorbent was characterized using FTIR and determination of point of zero charge (pHpzc) and surface function. Optimization of adsorption process was developed using central composite design (CCD) combined with response surface methodology (RSM) and artificial neural network (ANN). The input variables are pH, adsorbent dose, initial Cr(VI) concentration and phenol concentration. The adsorption capacity of the granular activated carbon towards Cr(VI) ions and phenol are the responses. Results of analysis of variance (ANOVA) identified the significance of various factors and their interaction. Optimum pH, adsorbent dose, initial Cr(VI) concentration and initial phenol concentrations were determinate using desirability function. RSM and ANN were compared by different statistical parameters. Results reveal that ANN has the best performance for prediction compared with RSM. Adsorption of Cr(VI) ions and phenol was affected by ionic strength. The potential of applicability of the adsorption process in treatment of real wastewater was evaluated by investigating the simultaneous adsorption of Cr(VI) ions and phenol onto activated carbon at optimum conditions.

Keywords: Activated carbon; Artificial neural network; Binary adsorption; Central composite design; Response surface methodology; Wastewater treatment

1. Introduction

The continuing progress of the industrial has largely contributed to environmental pollution problem by the fact that the industries involve huge quantity of toxic and hazardous chemicals that are used in different steps of processing. Effluents from industries contain a variety of organic and inorganic pollutants. Major inorganic pollutants are toxic metals such as hexavalent chromium (Cr(VI)) and the phenol is the important organic pollutants. Cr(VI) and phenol are frequently encountered together in many industrial wastewaters such as those coming from electroplating, leather tanning, textile, paints and pigments [1].

Chromium exists in water exclusively in the trivalent Cr(III) oxidation state or in the hexavalent Cr(VI) oxidation state [2]. Hexavalent chromium is 500 more toxic than the trivalent chromium [3] and it usually present in water as oxyanions such as chromate (CrO_4^{2-}) and dichromate ($Cr_2O_7^{2-}$). It is toxic for plants, animals and humans. Chronic toxicity of Cr(VI) in humans results in: lung cancer, kidney, liver and gastric damage [4]. Phenol is a priority pollutant due to its poor biodegradability, high toxicity to organisms even at low concentrations. Exposure to larger doses of phenol has been shown to cause gastrointestinal disorder, lung damage, liver disease, kidney disease, heart attack and finally can lead to death [5]. Due to the high toxicity of phenol and Cr(VI), they are subjected to specific regulations. World health organization (WHO) recommended 1 and 0.05 mg/L as the permissible phenol and Cr(VI) concentra-

*Corresponding author.

tion, respectively, in industrial discharge [6]. So it is necessary to reduce phenol and Cr(VI) in effluents to acceptable limits before discharge or reuse. In addition, any effort to propose solution for simultaneous removal of the two pollutants would be of value. Among various treatment methods for removal, adsorption process using activated carbon is a promising technique to reduce the level of the Cr(VI) and phenol in water. Activated carbon was the most widely used adsorbents due to its high adsorption capacity of broad range of pollutants, fast adsorption kinetic and its simplicity of design [7]. Many researches on the adsorption of compounds using various adsorbents have focused on removal of single compound but industrial effluents can contain various type of pollutant. So, it is necessary to study the simultaneous adsorption of pollutants.

Adsorption process is mainly influenced by the initial concentration of the adsorbate, the initial pH, the temperature, the contact time, the adsorbent characteristics and the agitation speed. In order to maximize the adsorption capacity, optimization of process variables is necessary. Conventional experiment design proceeds usually by varying one parameter by time and maintaining all other parameters constant. This is an inefficient and time consuming approach. It cannot also find the probable interactions between the variables. Result analysis is straightforward, but care must be taken in interpreting the results and multivariable modeling is impossible. These limitations are strongly resolved following the application of statistical experimental design such as response surface methodology (RSM) [8]. RSM is a useful statistical technique to predict the significance of various factors influencing the responses by varying them simultaneously [9]. Application of RSM leads to reduce the number of experiments in least time with low cost procedures [10,11]. RSM was employed for modeling the optimization of adsorption process [12–15].

Modeling the adsorption process can be also undertaken by the artificial neural networks (ANN) [16–18].

The aim of the present paper is to study the feasibility of using granular activated carbon as an adsorbent for the simultaneous adsorption of Cr(VI) and phenol from aqueous solutions. GAC was characterized using FTIR. Then the optimization of four operating parameters such as pH, adsorbent dose, initial Cr(VI) concentration and initial phenol concentration was performed using a RSM based on the central composite design. Significant factors and the interactions between them were identified and quantified using ANOVA and a second polynomial equation (regression model) describing the relationship between responses and independent parameters was proposed. On basis of the experimental data of CCD, a three layer ANN model was used to predict the simultaneous adsorption and subsequently compare the predictive performance offered by RSM and ANN. Effect of ionic strength was studied. The evaluation of performance of adsorbent in real water was investigated.

2. Materials and methods

2.1. Instruments and reagents

All chemicals without further purification including phenol, $K_2Cr_2O_7$, NaOH, HCl, NaCl, $NaNO_3$, Na_2SO_4 and KCl were supplied from Sigma Aldrich. Here, the salts were used as model to estimate the effect of ionic strength on the adsorption. Sodium hydroxide and chlorohydric acid were used to adjust the pH of solution using a Metrohm 780 pH meter. Stock solutions (1000 mg/L) of Cr(VI) and phenol were prepared by dissolving 2.834 g of $K_2Cr_2O_7$ and 1 g of phenol crystal in 1 L of deionized water and the working concentrations were prepared by its suitable dilution.

Concentration of Cr(VI) and phenol were measured by the diphenylcarbazide method and 4-aminoantipyrine method, respectively and were analyzed using a UV-Visible spectrophotometer (TOMOS V-1100 model). The concentration of chromium (VI) ions in the effluent was determined spectrophotometrically by using diphenyl carbazide as the complexing agent. The absorbance of the purple colored solution was read at 540 nm after 10 min. The concentration of residual phenol in the effluent was also determined spectrophotometrically. The absorbance of the colored complex of phenol with 4-aminoantipyrine was read at 510 nm after 5 min. No interference of chromium (VI) ions and phenol on the analysis method of the other pollutant was observed.

The adsorbent used was granular activated carbon GAC (NORIT 1240) purchased from Sigma Aldrich. Activated carbon was washed repeatedly with deionized water to remove the impurities, dried in an oven at 100°C to constant weight and then, stored in desiccators until use. Table 1 shows the main characteristics of GAC.

The identification and quantification of the surface functional groups of the GAC were carried out by the Bohem titration method [19]. First, 0.5 g of GAC was placed in 25 mL of 0.1 mol/L solutions of sodium hydroxide, sodium carbonate, sodium bicarbonate and hydrochloric acid. The sealed vials were shaken at room temperature for 24 h. Then each solution was filtrated and the excess base or acid was back-titrated with HCl or NaOH. The numbers of all acidic sites were calculated under the assumption that NaOH reacts with carboxylic groups, HCl reacts with basic surface functional groups, Na_2CO_3 reacts with carboxylic and lactonic groups and $NaHCO_3$ reacts only with carboxylic groups.

The pH of the point of zero charge was measured by the pH drift method [20].

Fourier transform infrared spectroscopy (FTIR in the range of 400–4000 cm^{-1}) of the adsorbent was recorded using FT-IR spectrophotometer (Model: Perkin Elmer). Spectra obtained were analyzed.

STATISTICA, a statistical package software version 10.0 was used to generate the matrix of experimental data of

Table 1
Main characteristics of GAC

Parameters	Values
Bulk density(g/cm^3)	0.5
Particle size (mm)	0.6–0.7
Moisture (%)	< 5
Ash (%)	12
BET surface area (m^2/g)	1100

CCD and to analyze the results of the experimental design. MATLAB 7 software was applied to train and test the ANN model.

2.2. Simultaneous adsorption of Cr(VI) and phenol experiments

A 200 mL round bottom flask with working volume of 100 mL was taken for the experiments and kept at 130 rpm and 25°C in a thermostatic bath. The effect of contact time on the simultaneous adsorption was studied at various contact times (5–180 min) as follows: a 0.5 g of adsorbent was added to a binary solution containing a 100 mg/L of Cr(VI) and 50 mg/L of phenol with adjusted pH. Then, batch experiments were carried for the optimization process according to the CCD. In each run, 100 mL of binary solution of Cr(VI) and phenol with adjusted adsorbate concentration, pH and adsorbent dose was shaken at fixed contact time and temperature. Then, solutions were filtered and analyzed for Cr(VI) and phenol.

Adsorption capacities for Cr(VI) and phenol (q_e, mg /g) on adsorbent were calculated by the following equation:

$$q_e = \frac{\left(C_{0,i} - C_{e,i}\right) \times V}{m} \tag{1}$$

where $C_{0,i}$ and $C_{e,i}$ are respectively the initial and equilibrium concentration (mg/L) of pollutant i (i.e., Cr(VI) or phenol) in the binary solution, V is the solution volume (L) and m indicates the adsorbent amount (g).

2.3. Central composite design

RSM, an experimental strategy of determination of optimum conditions of the process, has been applied in chemical engineering and sorption process optimization. CCD is one of the widely used forms of RSM. This method is suitable to fit the quadratic surface and to study the individual and interaction between parameters. The design was based on two-level full factorial design, which was augmented with center and star points. Total number of experiments of the designs (N) can be calculated as follows:

$$N = N_a + N_0 + N_c \tag{2}$$

where N_a is the number of experiments of the two level full factorial designs, N_0 is the number of center points and N_c is the number of star points.

In the present study, n was set at 4 so the number of experiments was 30 with 6 experiments were repeated in the center. The distance of the axial from center alpha ($\alpha = \left(2^n\right)^{1/4}$) depends on the number of points in the factorial portion of the design. Therefore, the value of α is equal to 2.

The behavior of system is explained by the following empirical second-order polynomial model:

$$Y = \beta_0 + \sum_{i=1}^{k} \beta_i X_i + \sum_{i=1}^{k} \beta_{ii} X_i^2 + \sum_{i=1}^{k-1} \sum_{j=2}^{k} \beta_{ij} X_i X_j \tag{3}$$

where Y is the predicted response, X_i and X_j are the independent variables, which affect the response Y, $X_i X_j$ are the interaction effects, β_0 is the intercept term, β_i , β_{ii} , β_{ij} are respectively the linear, quadratic and interaction coefficients.

2.4. Artificial neural networks

An artificial neural network (ANN) is a computational model inspired in the natural neurons.

Multilayer perceptron (MLP) is a feed forward ANN consisting of different layers of neurons including input, one or more hidden and output (Fig. 1). Each neurons of the first layer, which is called input layer, is connected to all of the neurons of the hidden layer. These neurons are also connected to the neurons of the output layer, which representing the output of the ANN.

In this study, a three layer ANN and Levenberg-Marquardt back propagation algorithm with 1000 iterations were applied for training the network. ANN's consist of four neurons of input layer (pH, adsorbent dose, initial Cr(VI) concentration and initial phenol concentration); two neurons of output layer (adsorption capacity of Cr(VI) and phenol) and 1–30 neurons of the hidden layer. For the two pollutants, all experimental data were divided into 70% for training, 15% for validation and 15% for testing the adequacy of model and prediction.

3. Results and discussion

3.1. Characterization of adsorbent

Results of the Boehm titration and the value of pH_{PZC} are illustrated in Table 2. According this table, the difference between the total acidic groups and the total basic groups is low and the pH_{PZC} was found to be 7.2.

FTIR spectrum of GAC is shown in Fig. 2. FTIR assignments of functional groups on adsorbent surface are listed in Table 3.

The FTIR spectrum of the GAC after the simultaneous adsorption of Cr(VI) and phenol are depicted in Fig. 2. FTIR studies of activated carbon after adsorption of both pollutant demonstrated that the strong band at 3441.6 cm^{-1} become weak. The change of the peak corresponding to the carbonyl group indicates the attachment of Cr(VI) and phenol with these functional groups.

3.2. Effect of contact time

The effect of contact time on simultaneous adsorption of Cr(VI) ions and phenol from binary solution onto granular activated carbon was studied at different time intervals (from 5 to 180 min) at room temperature, with an initial Cr(VI) concentration of 100 mg/L, an initial phenol concentration of 50 mg/L, a adsorbent dose of 5 g/L and an solution pH of 6. Results were displayed in Fig. 3. It was observed that the adsorption capacity of both adsorbates increases sharply with contact time and then gradually remains constant with increase in contact time and reached the equilibrium at 120 min for both adsorbates. The rapid adsorption at initial contact time is due to the availability of a large number of vacant sites then the slightly increase of adsorption capacity is due to the saturation of vacant sites.

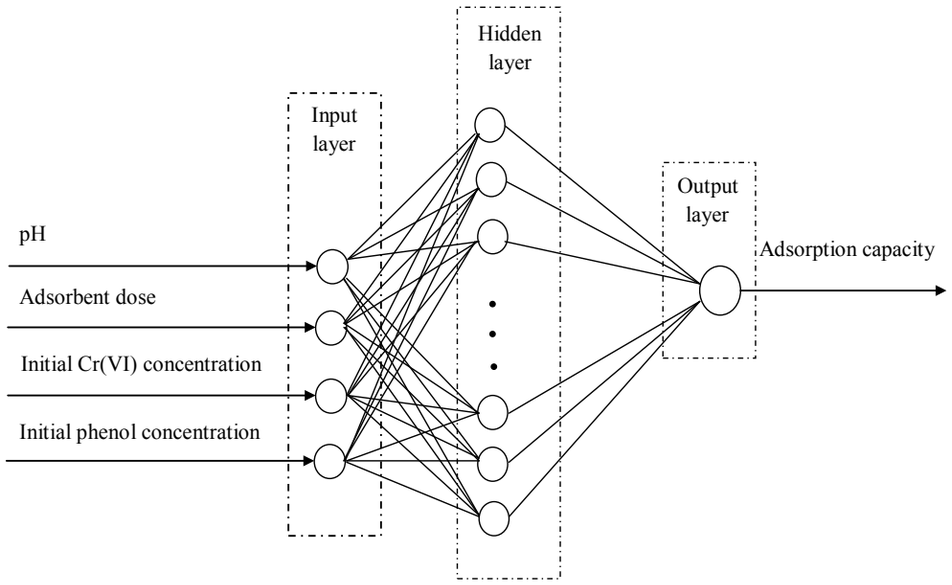

Fig. 1. Architecture of artificial neural network (ANN).

Table 2
Surface functional groups on the surface of GAC

Functions	Quantity (mmol/g)
Carboxylic	0.06
Lactone	0.04
Phenolic	0.04
Total acidity	0.14
Total basicity	0.2
pH_{PZC}	7.2

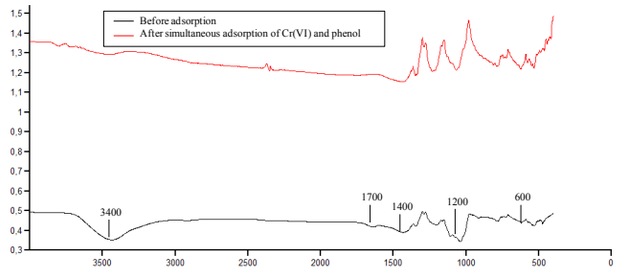

Fig. 2. FTIR spectrum of GAC.

Table 3
FTIR assignments of functional groups on adsorbent surface [21]

Adsorption bands (cm^{-1})	Assignment
3441.6	–OH stretching ($\nu_{(O–H)}$)
2800–2900	C–H stretching ($\nu_{(C–H)}$)
1679.6	C=O stretching $\nu_{(C=O)}$
1460	C–H bending $\delta_{(C–H)}$
1075	C–O stretching ($\nu_{(C–O)}$)
700–900	C–H bending aromatic rings $\delta_{(C–H)}$

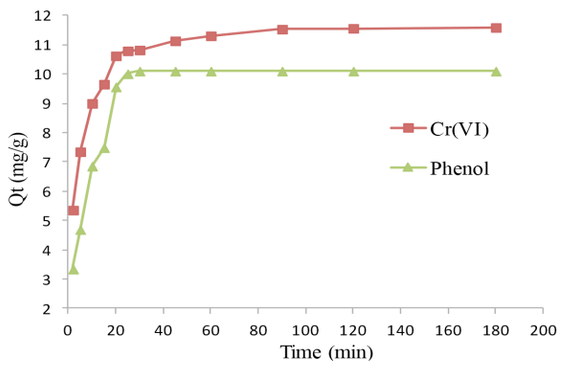

Fig. 3. The effect of contact time on the amount of adsorbed Cr(VI) and phenol (pH = 6, m_{GAC} = 0, 5 g, V = 100 mL, θ = 25°C, [Cr(VI)] = 100 mg/L, [Phenol] = 50 mg/L).

3.3. Optimization of simultaneous adsorption conditions using the RSM approach

Adsorption capacity of phenol and Cr(VI) ions were statistically studied as a function of the pH, adsorbent dose, initial Cr(VI) concentration and initial phenol concentration at a fixed contact time of 120 min.

Variables, experimental range and levels in coded factors (lowest (–α), low (–1), central (0), high (+1) and highest (+α)) are shown in Table 4.

For the RSM involving CCD, a total of 30 experiments was conducted for four factors at five levels with three replicates at center point. The number of experiments required (N) is given by the expression: 2^k (2^4 = 16; star

points) + 2 k (2 × 4 = 8; axial points) + 6 (center points; 6 replications). Experimental design matrix together with the value of observed and predicted responses (adsorption capacity of Cr(VI) and adsorption phenol capacity) are listed in Table 5.

Table 4
Central composite design analysis

Variables, units	Range and levels (coded)				
	−α	–1	0	+1	+α
pH	2	4	6	8	10
Adsorbent dose (g)	0.5	0.75	1	1.25	1.5
Initial Cr(VI) concentration (mg/L)	100	150	200	250	300
Initial phenol concentration (mg/L)	50	75	100	125	150

3.3.1. Development of regression model equation

Results of experimental design were analyzed using the STATISTICA software to investigate the main effect of factors, the interactions, the coefficient standard deviations and various statistical parameters. These parameters are shown in Table 6 for the adsorption capacity of Cr(VI) and the adsorption capacity of phenol, respectively.

It was observed from table 6 that the values of constant for the responses Y1 and Y2 were found to be 6.992 and 10.059 respectively and were significant (P = 0.0000). The constant, which are independent of the factors and their interactions, shows that the average adsorption capacity of Cr(VI) and phenol were 6.9926 mg/g and 10.05939 mg/g, respectively.

Linear effect of pH, adsorbent dose and initial Cr(VI) concentration were highly significant on the adsorption capacity of Cr(VI). All quadratic terms were found to

Table 5
RSM design and its observed and predicted values

Run order	pH	Adsorbent dose	Initial Cr(VI) concentration	Initial phenol concentration	Adsorption capacity Cr(VI) (mg/g)		Adsorption capacity phenol (mg/g)	
					Observed	Predicted	Observed	Predicted
1	8	0.75	250	125	16.542	14.562	16.599	17.115
2	4	1.25	250	125	20.797	20.539	6.675	7.568
3	8	0.75	150	75	6.552	6.429	10.103	9.692
4	4	1.25	150	75	9.971	11.551	5.702	5.665
5	6	1	200	100	6.410	6.993	10.058	10.059
6	8	1.25	150	125	1.082	2.001	9.959	10.016
7	8	1.25	250	75	9.458	8.408	6.026	6.290
8	6	1	200	100	6.698	6.993	10.058	10.059
9	4	0.75	250	75	28.679	27.379	9.682	10.106
10	4	0.75	150	125	14.909	15.578	16.719	16.935
11	6	1	200	100	6.700	6.993	10.067	10.059
12	4	1.25	150	125	9.743	8.464	10.031	9.037
13	4	1.25	250	75	20.284	19.135	6.112	5.060
14	4	0.75	150	75	16.904	17.553	10.139	10.128
15	8	1.25	150	75	3.703	5.060	6.116	6.019
16	6	1	200	100	7.122	6.993	10.013	10.059
17	8	0.75	250	75	11.965	12.018	10.187	10.547
18	8	0.75	150	125	4.558	4.481	16.707	17.125
19	8	1.25	250	125	11.715	9.839	10.046	9.423
20	4	0.75	250	125	23.478	29.895	16.586	16.049
21	6	1	200	100	7.262	6.993	10.076	10.059
22	2	1	200	100	21.652	22.686	6.747	7.221
23	6	1	100	100	6.623	3.974	10.139	10.493
24	6	1	200	100	7.763	6.993	10.081	10.059
25	6	1	300	100	17.378	21.639	10.076	9.879
26	6	1	200	150	14.387	16.808	15.083	15.034
27	6	0.5	200	100	15.390	16.925	20.153	19.591
28	6	1.5	200	100	6.125	6.201	6.717	7.436
29	6	1	200	50	18.162	17.352	4.889	5.094
30	10	1	200	100	0.284	0.862	8.958	8.640

Table 6
Estimated regression coefficients for adsorption capacity of Cr(VI) and phenol

Factor	Cr(VI)					Phenol				
	Coef	SEcoef	t	P	Remarks	Coef	SE coef	t	P	Remarks
Constant	6.992	0.833	8.386	0.0000	*	10.059	0.257	39.00	0.0000	*
X_1	–5.455	0.416	–13.086	0.0000	*	0.354	0.128	2.751	0.0148	*
X_2	–2.681	0.416	–6.430	0.0000	*	–3.038	0.128	–23.563	0.0000	*
X_3	4.416	0.416	10.592	0.0000	*	–0.153	0.128	–1.191	0.2519	–
X_4	–0.135	0.416	3.726	0.7489	–	2.485	0.128	19.270	0.0000	*
X_1^2	1.195	0.390	3.064	0.0078	*	–0.532	0.120	–4.411	0.0005	*
X_2^2	1.142	0.390	2.929	0.0103	*	0.863	0.120	7.157	0.0000	*
X_3^2	1.453	0.390	–0.325	0.0020	*	0.031	0.120	0.262	0.7967	–
X_4^2	2.521	0.390	6.466	0.0000	*	0.001	0.120	0.009	0.9923	–
$X_1 X_2$	1.158	0.510	2.268	0.0384	*	0.197	0.157	1.249	0.2306	–
$X_1 X_3$	–1.059	0.510	–2.074	0.0556	–	0.219	0.157	1.387	0.1855	–
$X_1 X_4$	0.006	0.510	0.013	0.9894	–	0.156	0.157	0.989	0.3380	–
$X_2 X_3$	–0.560	0.510	–1.097	0.2896	–	–0.145	0.157	–0.923	0.3701	–
$X_2 X_4$	–0.278	0.510	–0.544	0.5941	–	–0.858	0.157	–5.438	0.0000	*
$X_3 X_4$	1.122	0.510	2.198	0.0440	*	–0.216	0.157	–1.368	0.1913	–

*Significant

be significant. However, linear effect of initial phenol concentration and all interaction except X_1X_2 and X_3X_4 were insignificant to adsorption capacity of Cr(VI). For adsorption capacity of phenol, the analysis indicated those linear, quadratic terms of adsorbent dose and linear terms of initial phenol concentration imposed the greatest effect (P = 0 for all). Moreover, linear and quadratic effect of pH and X_2X_4 interaction had a significant effect (P < 0.005). All other interaction, quadratic effect of initial phenol concentration and both linear and quadratic effect of initial Cr(VI) concentration were considered insignificant.

Second-order polynomial equations for the adsorption capacity (Y1) of Cr(VI) and the adsorption capacity (Y2) of phenol in terms of coded factors are given by:

$$Y1 = 6.992 - 5.455X_1 - 2.681X_2 + 4.416X_3 - 0.135X_4 + 1.195X_1^2 + 1.142X_2^2 + 1.453X_3^2 + 2.251X_4^2 + 1.158X_1X_2 - 1.059X_1X_3 + 0.006X_1X_4 - 0.560X_2X_3 - 0.278X_2X_4 + 1.122X_3X_4 \quad (4)$$

$$Y2 = 10.059 - 0.354X_1 - 3.038X_2 - 0.153X_3 + 2.485X_4 - 0.532X_1^2 + 0.863X_2^2 + 0.031X_3^2 + 0.011X_4^2 + 0.197X_1X_2 + 0.219X_1X_3 + 0.156X_1X_4 - 0.145X_2X_3 - 0.858X_2X_4 - 0.216X_3X_4 \quad (5)$$

From Eqns. (4) and (5), it can be seen that pH, adsorbent dose and initial phenol concentration have a negative effect but the initial Cr(VI) concentration had a positive effect on the adsorption capacity of Cr(VI). In addition, pH and initial phenol concentration have a positive effect but the initial Cr(VI) concentration and adsorbent dose have a negative effect on the adsorption capacity of phenol. A positive value represents a synergistic effect, while a negative value indicates an antagonistic effect.

3.3.2. Analysis of variance study

The adequacy and the significance of statistical model were evaluated through analysis of variance (ANOVA); thus, ANOVA was performed for simultaneous adsorption of Cr(VI) and phenol onto granular activated carbon and its results are provided in Table 7. F-value and p-value can measure the effectiveness of the model. The calculated F-value for all effect was compared with the critical F value ($F_{0.05.df.(n-df+1)}$) for the considered probability (p = 0.05) and degrees of freedom. Since, for 1 degree freedom and n = 30, $F_{0.05.df.(n-df+1)}$ is equal to 4.17. Each variable or interaction between variables has an F-value greater than 4.17 and p value smaller or equal to 0.05 are significant.

The fitting of the model was evaluated by the determination coefficient (R^2) and adjusted R^2. Values of R^2 were 0.96351 and 0.98597 for the adsorption capacity of Cr(VI) and phenol, respectively. This results meaning that the 96.351% and 98.597% of the variation for adsorption capacity of Cr(VI) and phenol respectively, are explained by the applied model. Adjusted R^2 corrects the value of R^2 for the sample size and the number of terms in the model. Values of adjusted R^2 were found to be 0.92945 and 0.97287 for the adsorption capacity of Cr(VI) and phenol, respectively. The difference between R^2 and corresponding adjusted R^2 was not significant indicating a high correlation between the experimental and predicted response.

Experimental and predicted data for adsorption capacity of Cr(VI) and phenol plot is presented in Fig. 4. It indicated that experimental data and predicted value obtained from the model were in good agreement. These results indicate that the simultaneous adsorption of Cr(VI) and phenol onto granular activated carbon is statistically validated over the range of considered experimentation for the adsorption capacity response.

Table 7
ANOVA for the quadratic equations for adsorption capacity of Cr(VI) and phenol

Factor	Cr(VI)					Phenol				
	SS	d.f	M.S	F-value	P-value	SS	d.f	M.S	F-value	P-value
X_1	714.430	1	714.4301	171.246	0.0000*	3.0218	1	3.0218	7.5708	0.0148*
X_2	39.182	1	39.1815	41.351	0,0000*	39.182	1	39.182	555.224	0.0000*
X_3	172.515	1	172.5153	112.193	0.0000*	2221.6074	1	2221.6074	1.419	0.2519
X_4	35.802	1	35.8020	0.106	0.7489	20.4495	1	20.4495	371.346	0.0000*
X_1^2	468.066	1	468.0660	9.391	0.0078*	0.5667	1	0.5667	19.464	0.0005*
X_2^2	57.938	1	57.9383	8.581	0.0103*	0.0274	1	0.0274	51.234	0.0000*
X_3^2	0.443	1	0.4431	13.887	0.0020*	148.2161	1	148.2161	0.068	0.7967
X_4^2	174.426	1	174.4262	41.809	0.0000*	0.0000	1	0.0000	0.0001	0.9923
$X_1 X_2$	21.469	1	21.4687	5.145	0.0384*	0.6231	1	0.6231	1.561	0.2306
$X_1 X_3$	17.948	1	17.9477	4.301	0.0556	0.7684	1	0.7684	1.925	0.1855
$X_1 X_4$	0.001	1	0.0008	0.002	0.9894	0.3908	1	0.3908	0.979	0.3380
$X_2 X_3$	5.027	1	5.0273	1.205	0.2896	0.3407	1	0.3407	0.853	0.3701
$X_2 X_4$	1.237	1	1.2367	0.296	0.5941	11.8032	1	11.8032	29.572	0.0000*
$X_3 X_4$	20.169	1	20.1689	4.834	0.0440*	0.7474	1	0.7474	1.872	0.1913
Error	62.579	15	4.171			5.986	15	0.399		
Total SS	1714.930	29				426.6017	29			

*Significant

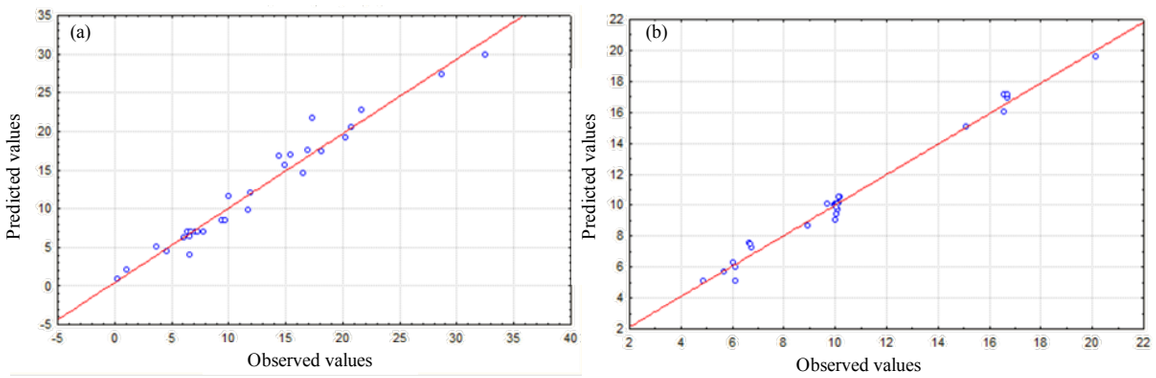

Fig. 4. Scatter plot of RSM model predicted values versus actual values for CCD matrix for Cr(VI) (a) and phenol (b).

3.3.3. Effect of variables and response surface 3D plots

The use of 3D response surface plot for the regression model is highly recommended for the graphical interpretation of interactions of variables [22]. Figs. 5a–c show 3D surface of adsorption capacity of Cr(VI) and adsorption capacity of phenol versus significant interaction of variables while the other two were fixed constant. According to ANOVA table, interactions X_1X_2, X_2X_4 and X_3X_4 for simultaneous removal of Cr(VI) and phenol were significant.

Fig. 5a shows interactive effect of pH and adsorbent dose on adsorption capacity of Cr(VI). Adsorption capacity decrease with enhance in adsorbent dosage due to a reduction of the instauration of the adsorption sites through the adsorption reaction [23]. This figure reveals also that the adsorption capacity of Cr(VI) decrease with the increase of pH of solution. Maximum adsorption capacity was observed under acidic condition. At low pH, the dominant form of Cr(VI) was $Cr_2O_7^{2-}$ and $HCrO_4^-$. In addition, the GAC surface is positively charged. Therefore, there is a strong electrostatic attraction between the surface of adsorbent and $Cr_2O_7^{2-}$ and $HCrO_4^-$ anions [24]. At high value of pH, Cr(VI) is present in form of $Cr_2O_7^{2-}$ and the ion OH^- is predominated, adsorption capacity decrease. This can be attributed to the competition between the both anions to be adsorbed in the surface of adsorbent [25]. At high pH, the surface is also negative charged which is not favorable for anion adsorption.

Fig. 5b shows interaction effect of initial phenol concentration and initial concentration of Cr(VI) concentration on the adsorption of Cr(VI). The increase of the adsorption capacity with the increase of the initial concentration of Cr(VI) could be due to the greater mass transfer driving force [26]. In contrast, the adsorption capacity increases with the increase of the initial concentration of phenol.

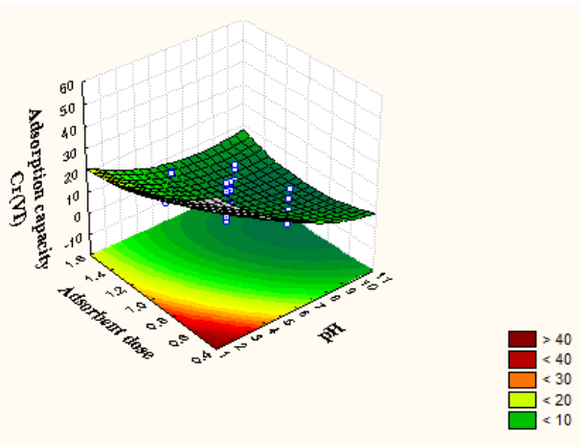

(a)

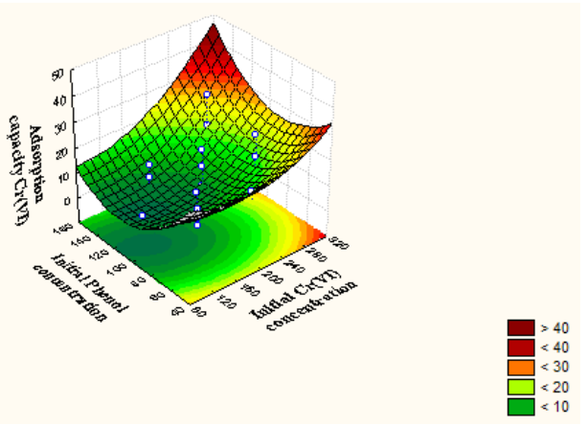

(b)

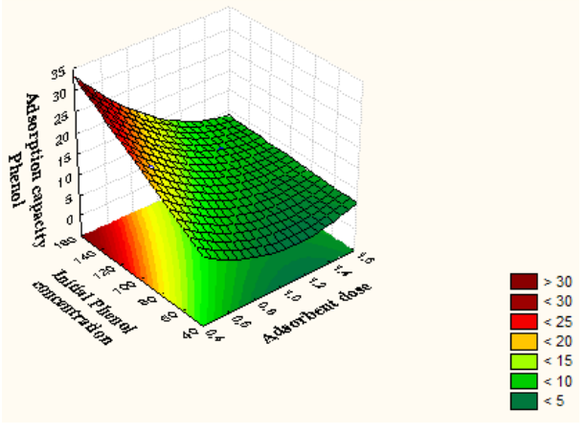

(c)

Fig. 5. Response surfaces plots of interactions X_1X_2 for Cr(VI) (a), X_3X_4 for Cr(VI) (b) and X_2X_4 for phenol(c).

Adsorption capacity of phenol increased with the increase of phenol concentration and decreased with the increase of the adsorbent dose (Fig. 5c).

3.3.4. Optimization using the desirability function

Desirability function approach is a technique for the simultaneous determination of the level of input variables that can produce the optimum one or more response. Each response is transformed into a desirability value d and the total desirability function D, which is the geometric mean of the individual desirability values, is computed and optimized. The corresponding desirability will lie between 0 and 1. If the response is on target then the desirability value will be equal to 1 and if the response is outside an acceptable region the desirability value equal to 0. The profile for predicted values and desirability option in

STATISTICA software is used for the optimization process. The overall desirability must be maximized to find the best and efficient combination of levels of input variables. CCD optimization design matrix (Fig. 6) show that maximum adsorption capacity of Cr(VI) (33.92 mg/g and desirability of 1.0) and adsorption capacity of phenol (20.27 mg/g with desirability of 1.0) was achieved at following conditions: pH (8), adsorbent mass (0.75 g), initial Cr(VI) concentration (300 mg /L) and initial phenol concentration (150 mg/L).

3.3.5. Verification of optimized conditions and predictive model

To confirm the validity of the model and optimization procedure, three additional experiments were conducted under optimum conditions. Results were compared to predicted values of responses using the model equation. Table 8 reports the mean value of experimental response. The difference between predicted and experimental values is negligible. This means that the efficiency of both proposed models to predict Cr(VI) and phenol adsorption capacities, under specified range of adsorption process variables, are effective.

3.4. Optimization of simultaneous adsorption conditions using the ANN approach

In this work, ANN was used to predict adsorption capacity of Cr(VI) and phenol through an experimental design CCD. ANN has four inputs, one hidden layer (with n neurons) and two outputs. Optimal number of neurons of the hidden layer was determinate by training various ANN topologies and comparing the performance of these networks using the mean square errors (MSE) and coefficient of determination (R^2), which can be defined as follows:

$$MSE = \frac{1}{N}\sum_{i=1}^{N}\left(\left|Yprd,i - Yexp,i\right|\right)^2 \quad (6)$$

$$R^2 = 1 - \left(\frac{\sum_{i=1}^{n}\left(Yprd,i - Yexp,i\right)^2}{\sum_{i=1}^{n}\left(Yprd,i - Ym\right)^2}\right) \quad (7)$$

The number of neurons was obtained by testing a different number of neurons, in the range of 1–30, in the hidden layer and selecting the optimal one based on the minimum value of MSE and maximum value of R^2. Table 9 represents the dependence between neuron numbers at hidden layer with MSE and R^2.

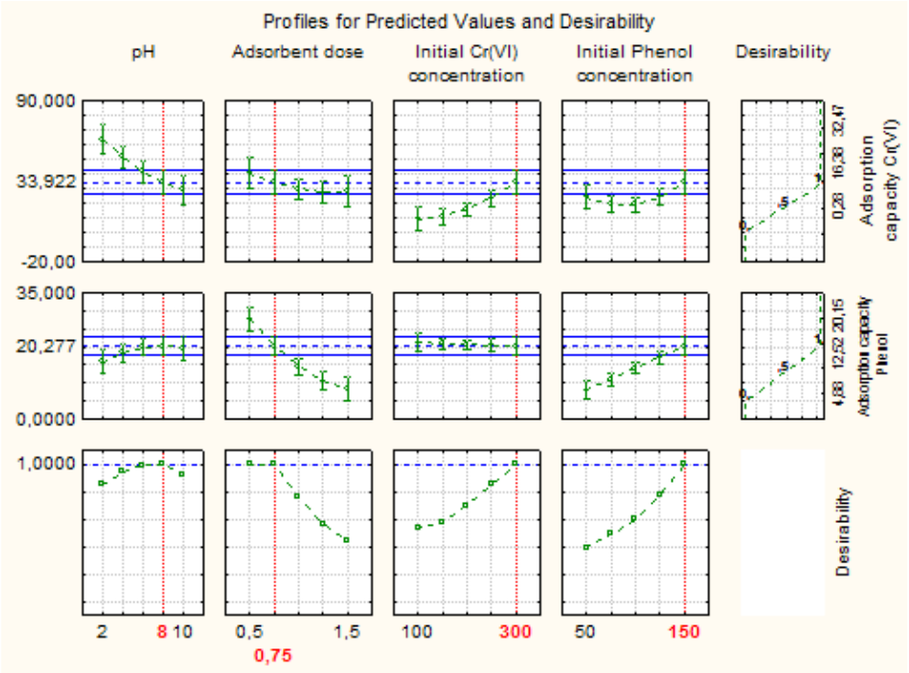

Fig. 6. The profile of desirability function.

Table 8
Predicted and experimental value of adsorption capacity at optimum conditions

pH	8
Adsorbent dose (g/100 mL)	0.75
Initial Cr(VI) concentration (mg/L)	300
Initial phenol concentration (mg/L)	150
Adsorption capacity Cr(VI) (mg/g)	
Predicted	35.149
Experimental	33.922
Adsorption capacity phenol (mg/g)	
Predicted	19.601
Experimental	20.277

From the results of Table 9, we can see that the best structure of ANN was obtained with 7 and 5 neurons at the hidden layer with minimum value of MSE ($3.016\ 10^{-02}$ for training and 2.087 for testing, $3.500\ 10^{-09}$ for training and $8.888\ 10^{-09}$ for testing) and maximum value R^2 (0.9997 for training and 0.9804 for testing, 0.9999 for training and 0.9999 for testing) for the Cr(VI) and phenol, respectively.

The adsorption capacity of Cr(VI) and phenol predicted by ANN versus to experimental data is presented in Fig. 7.

These plots show a good fit between experimental values of both adsorption capacity and those predicted by ANN model. High values of coefficient of determination (0.991 for Cr(VI) and 1 for phenol) illustrate reliability of ANN models.

3.5. Comparison between RSM and ANN

Performance of the RSM and ANN was evaluated by comparing the statistical parameters such as the coefficient of determination (R^2), the root mean square errors (RMSE), mean absolute errors (MAE) and the absolute average deviation (AAD).

$$RMSE = \sqrt{\frac{1}{N}\sum_{i=1}^{N}\left(\left|Yprd,i - Yexp,i\right|\right)^2} \tag{8}$$

$$MAE = \frac{1}{N}\sum_{i=1}^{N}\left|Yprd,i - Yexp,i\right| \tag{9}$$

$$AAD\ \% = \left(\frac{1}{N}\sum_{i=1}^{N}\frac{\left|Yprd,i - Yexp,i\right|}{Yprd,i}\right)\times 100 \tag{10}$$

where N is the number of sample points, $Y_{prd,i}$ is the predicted response and $Y_{exp,i}$ is the experimentally determined response.

Table 10 presents statistical comparison of RSM and ANN models. The coefficient of determination R^2, which is a number that indicates how well data fit a statistical model, must be closed to 1.0. In contrast the absolute average deviation (AAD), which is the average distance between experimental and predicted data, must be as small as possible.

The value of R^2 and of AAD% for both adsorbates confirms that the ANN model is superior in predicting the adsorption capacity. This is confirmed by the values of RMSE and MAE which are less for ANN than for RSM for

Table 9
Dependence between neuron numbers at hidden layer with MSE and R^2

Number of neurons	Cr(VI)				Phenol			
	Train		Test		Train		Test	
	MSE	R^2	MSE	R^2	MSE	R^2	MSE	R^2
1	18.005	0.7491	35.083	0.4188	$1.072\ 10^{-07}$	0.9999	$1.240\ 10^{-07}$	0.9999
2	5.051	0.9383	24.144	0.5693	$7.263\ 10^{-08}$	0.9999	$2.286\ 10^{-03}$	0.9999
3	11.151	0.9039	11.703	0.9686	$2.685\ 10^{-08}$	0.9999	1.107 10-02	0.9989
4	2.883	0.9969	19.556	0.8285	$7.031\ 10^{-01}$	0.9855	$7.229\ 10^{-01}$	0.9847
5	2.060	0.9829	5.224	0.9308	$3.500\ 10^{-09}$	0.9999	$8.888\ 10^{-09}$	0.9999
6	7.012	0.9232	31.860	0.5481	$4.182\ 10^{-08}$	0.9999	$2.499\ 10^{-01}$	0.9956
7	$3.016\ 10^{-02}$	0.9997	2.087	0.9804	$2.529\ 10^{-01}$	0.9944	$1.591\ 10^{-01}$	0.9949
8	$5.992\ 10^{-02}$	0.9993	29.796	0.9571	$7.084\ 10^{-05}$	0.9999	$4.004\ 10^{-04}$	0.9999
9	2.678	0.9710	12.458	0.0248	$1.104\ 10^{-06}$	0.9999	$6.599\ 10^{-01}$	0.9911
10	12.306	0.9292	11.682	0.8051	$4.335\ 10^{-07}$	0.9999	1.7730	0.9696
13	5.496e-02	0.9994	15.370	0.9321	$6.366\ 10^{-10}$	0.9999	$2.553\ 10^{-03}$	0.9999
15	$3.371\ 10^{-01}$	0.9965	45.676	0.4720	$3.919\ 10^{-02}$	0.9991	15.008	0.9281
20	9.241	0.9505	101.455	0.7128	$1.705\ 10^{-01}$	0.9961	$2.705\ 10^{-01}$	0.9976
25	8.256	0.9446	56.449	0.8264	$2.057\ 10^{-06}$	0.9999	$6.521\ 10^{-07}$	0.9999
30	5.939	0.9471	136.882	0.6211	$5.019\ 10^{-05}$	0.9999	$9.528\ 10^{-02}$	0.9942

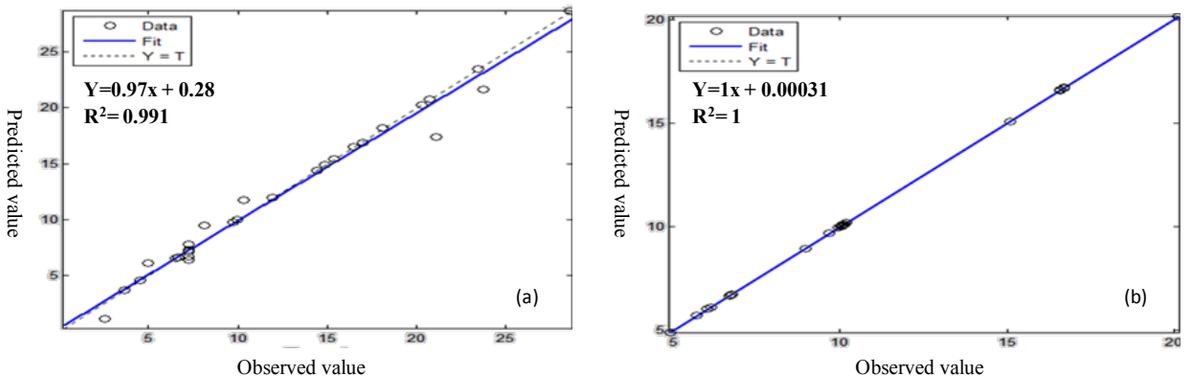

Fig. 7. Scatter plot of ANN model predicted values versus actual values for CCD matrix for Cr(VI) (a) and phenol (b).

Table 10
Evaluation of ANN and RSM models

Models	Statistical parameters							
	R^2		RMSE		MAE		AAD%	
	Cr(VI)	Phenol	Cr(VI)	Phenol	Cr(VI)	Phenol	Cr(VI)	Phenol
ANN	0.991	1	0.219	0.0031	0.173	0.0031	3.485	0.0033
RSM	0.963	0.985	1.799	0.446	1.214	0.329	13.766	3.757

both pollutants. In fact, this finding is consistent with other research comparing the both methodologies [27,28]. But RSM offers to study the linear, quadratic and interaction effect and to reduce the number of experiments, cost and time as compared to ANN.

3.6. Kinetic study

Kinetic modeling is important to know the nature of adsorption process. Different kinetic models including pseudo-first-order and the pseudo-second-order kinetic and intraparticle diffusion model were applied to evaluate

the mechanism of adsorption and rate limiting steps such as chemical reaction, diffusion control and mass transport processes. The linear form of pseudo-first-order [29], pseudo-second-order [30] and intraparticle diffusion [31] equations are expressed as:

$$\log\left(q_e - q_t\right) = \log q_e - \frac{k_1}{2.303}t \tag{11}$$

$$\frac{t}{q_t} = \frac{1}{k_2 q_e^2} + \frac{t}{q_e} \tag{12}$$

$$q_t = K_{dif}t^{1/2} + C \tag{13}$$

where q_e and q_t are the adsorption capacities (mg/g) at equilibrium and at time t, respectively. k_1 (1/min), k_2 (g/mg min) and k_{dif} (mg/g min$^{0.5}$) are the rate constants.

The kinetic adsorption parameters were determined using binary solutions at a concentration of adsorbent (0.5 g). The estimated kinetic models for Cr(VI) and phenol are shown in Table 11. As can be seen, the second order kinetic model generated the higher value of correlation coefficient R^2 (R^2 >0.99 for Cr(VI) and phenol) which show that this model better fitted to the experimental data than the first order kinetic model. The theoretical $q_{e(cal)}$ values were very close to the experimental data. This implies a high efficiency of this model for the explanation of data.

According to intraparticle diffusion the plot of adsorption capacity q_t vs. $t^{1/2}$ was drawn. If the plot is a straight line (C = 0), the intra particle diffusion is involved, but here plot for the two pollutants does not pass through origin which indicated some other mechanism along with intraparticle diffusion is also involved.

3.7. Isotherm study

In order to optimize the adsorption process parameters, Langmuir and Freundlich isotherm models were used to analyze the experimental data. For isotherm studies, single and binary solutions with various concentrations of Cr(VI) (100, 150, 200, 250 and 300 mg/L) and phenol (50, 75, 100, 125 and 150 mg/L) which are around the optimal points were investigated with 0.5 g of adsorbent at 298K.

Table 11
Kinetic parameters for the simultaneous removal of Cr(VI) and phenol from multi-component system

Models	Parameters	Cr(VI)	Phenol
First order kinetic model	k_1 (1/min)	0.078	2.377
	$q_{e(cal)}$ (mg/g)	1.822	0.135
	R^2	0.946	0.863
Second order kinetic model	k_2 (g/mg min)	0.039	0.032
	$q_{e(cal)}$ (mg/g)	11.627	10.277
	R^2	0.999	0.999
Intraparticule diffusion	k_{dif} (mg/g min$^{0.5}$)	0.255	0.366
	C (mg/g)	8.338	6.113
	R^2	0.466	0.469
Experimental data	$q_{e(exp)}$ (mg/g)	11.595	10.013

The Langmuir isotherm [32] is valid for monolayer sorption on specific homogeneous sites within the adsorbent and once adsorbate molecule occupies a site and presented by the following equation:

$$\frac{C_e}{q_e} = \frac{1}{K_L Q_m} + \frac{C_e}{Q_m} \tag{14}$$

where C_e is the concentration of the phenol solution (mg/L) at equilibrium, q_e is the amount of adsorbate adsorbed per unit mass of adsorbent at equilibrium (mg/g), q_m and K_L are the maximum adsorption capacity (mg/g) and the Langmuir constant (L/mg), respectively.

In order to determine if the adsorption process is favorable or unfavorable, a dimensionless constant separation factor or equilibrium parameter R_L, is defined according to the following equation [33]:

$$R_L = \frac{1}{1 + K_L C_0} \tag{15}$$

where K_L is the Langmuir constant (L/mg) and C_0 is the initial phenol concentration (mg/L). The value of R_L indicates the type of isotherm to be favorable ($0 < R_L < 1$), linear ($R_L = 1$), unfavorable ($R_L > 1$), or irreversible $R_L = 0$.

The Freundlich isotherm is an empirical equation assuming that the adsorption process takes place on a heterogeneous surface through a multilayer adsorption mechanism [34]. The Freundlich equation can be given by the equation:

$$\ln q_e = ln\ K_F + \frac{1}{n}\ln C_e \tag{16}$$

where K_F (L/mg) and n are indicators of adsorption capacity and adsorption intensity, respectively. $1/n$ values indicate the type of isotherm to be irreversible ($1/n = 0$), favorable ($0 < 1/n < 1$), unfavorable ($1/n > 1$).

The isotherm parameters and linear regression coefficient (R^2) values for single and binary system are shown in Table 12. The results indicated that Freundlich isotherm was best agreed with experimental data having higher values of R^2 for both Cr(VI) and phenol than the Langmuir isotherm. This means that the adsorption of Cr(VI) and phenol takes place at heterogeneous surface and as a multi-layer adsorption onto GAC surface.

3.8. Effect of the ionic strength

Adsorption process might be affected by the presence of dissolved salts in the aqueous solutions, so the effect of salinity on the simultaneous adsorption of Cr(VI) and phenol was studied. In binary solutions containing 150 mg/L of Cr(VI) and 75 mg/L of phenol were added different types of salts at different concentrations. Fig. 8 shows the effect of ionic strength on the adsorption capacity of both adsorbates.

The capacity of adsorption of Cr(VI) decrease with the increase of ionic strength. This trend can be explained attributed to the competition between anions of salts and hydrochromate ion ($HCrO_1^-$) for surface site [35]. In contrast, the adsorption capacity of phenol increases with increasing

Table 12
Parameters of different isotherms for Cr(VI) and phenol for single and multi-component system

Isotherm models	Parameters	Cr(VI) single	Cr(VI) multi	Phenol single	Phenol multi
Langmuir	Q_m (mg/g)	104.166	52.631	277.777	46.728
	K_L (L/mg)	0.366	0.496	0.012	0.420
	R^2	0.975	0.926	0.931	0.977
	R_L	0.025–0.008	0.019–0.006	0.6219–0.039	0.044–0.015
Freundlich	$1/n$	0.969	0.726	0.530	0.593
	K_F (L/mg)	2.671	1	8.908	13.570
	R^2	0.973	0.960	0.991	0.900

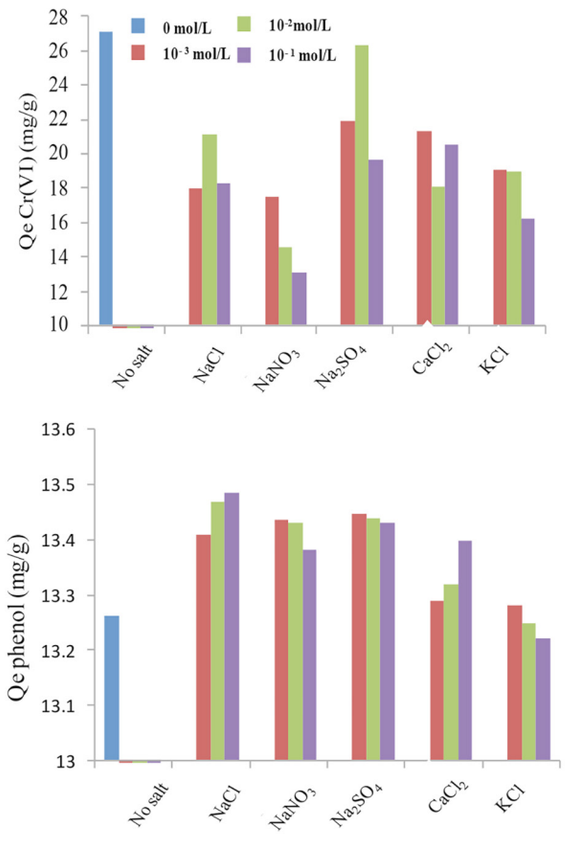

Fig. 8. Effect of ionic strength (pH = 6, m_{GAC} = 0.5 g, V = 100 mL, T = 25°C, [Cr(VI)] = 150 mg/L, [Phenol] = 75 mg/L).

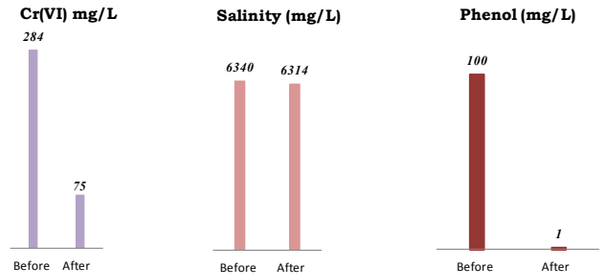

Fig. 9. Removal of Cr(VI) and phenol from a tannery wastewater (pH = 8, m_{GAC} = 0.75 g, V = 100 mL, T = 25°C).

Table 13
Comparison of the maximum adsorption capacity of phenol and Cr(VI) onto various adsorbents

Adsorbent	Maximum adsorption capacities(mg/g)		References
	Cr(VI)	Phenol	
Activated carbon (tea waste biomass)	199.523 mg/g	9.487 mg/g	[37]
Bacillus sp. immobilized onto the surface of tea waste biomass	741.389 mg/g	7.761 mg/g	[38]
GAC(NORIT 1240)	52.631	46.728	This work

ionic strength which may due to the salting out effect. This phenomenon reduces the solubility of the non-electrolyte in water (phenol) at high salt concentration and thus intensifies their diffusion in adsorbent [36].

3.9. Application in real water samples

The efficacy of GAC, as an adsorbent, for simultaneous removal of Cr(VI) and phenol was evaluated by treating it with a real industry effluent sample. Effluent was collected from a tannery industry. The composition of effluent sample is: Cr(VI): 284 mg/L, phenol: 100 mg/L, salinity: 6340 mg/L and pH 12.37. Typically, after adjustment of pH to 8, a 0.75g of GAC was mixed with 100 mL of wastewater for 2 hours and after filtration, final concentration of Cr(VI) and phenol were determined. Fig. 9 shows the concentration of both pollutants and the salinity before and after the adsorption process.

The residual concentration of Cr(VI) and phenol after treatment were 75 mg/L and 1 mg/L, which correspond in terms of adsorption capacity of 27.76 mg/g and 13.24 mg/g. These results suggest that the GAC can be effectively used for the simultaneous removal of the two pollutants from real water.

3.10. Comparative study

The sorption capacities of Cr(VI) and phenol on GAC were compared with other previously adsorbents reported in the literature as given in Table 13.

4. Conclusion

In this study the potentiel of granualr activated carbon, as an adsorbant, for simultaneous Cr(VI) and phenol uptake was investigated. Characterization of this adsorbent was carried using boehm titration, determination of pHpzc and FTIR analysis. RSM and ANN were utilized for the optimization of the simultaneous adsorption process. CCD under RSM was used to investigated the impact of four factors (pH, adsorbent dose, initial Cr(VI) concentration and initial phenol concentration) and their interaction on simutaneous adsorption of Cr(VI) and phenol from aqueous solution. The highest adsorption capacity of Cr(VI) (33.92 mg/g) and phenol (20.27 mg/g) was achieved under optimum conditions determinated using desirability function: pH (8), adsorbent mass (0.75 g), initial Cr(VI) concentration (300 mg/L) and initial phenol concentration (150 mg/L). The second-order polynomial model for Cr(VI) and phenol present an acceptable determination coefficient of 0.963 and 0.985, respectively. In addition, the modeling of simultaneous adsorption process was studied using ANN with 7 neurons for Cr(VI) and 5 neurons for phenol in the hidden layer using a back propagation algorithm. The comparison between both models reveals that ANN was superior to the RSM in terms of the coefficient of determination (R^2), root mean square errors (RMSE), mean absolute errors (MAE) and absolute average deviation (AAD). Ionic strength has an effect on the uptake of both adsorbates. The adsorbent has been successfully applied in real water.

References

[1] J.W. Patterson, Industrial Wastewater Treatment Technology, Butterworth Publishers, Stoneham, MA (1985) 53–393.

[2] U. Thacker, R. Parikh, Y. Shouche, D. Madamwar, Hexavalent chromium reduction by Providencia sp., Process Biochem., 41 (2006) 1332–1337.

[3] J. Yao, L. Tian, L.Y. Wang, A. Djah, F. Wang, H. Chen, E. Bramanti, Microcalorimetric study the toxic effect of hexavalent chromium on microbial activity of Wuhan brown sandy soil: an in vitro approach. Ecotoxicolo. Environ. Saf., 69 (2008) 289–295.

[4] M. Cieślak-Golonka, Toxic and mutagenic effect of chromium (VI). A review, Polyhedron, 15 (1996) 3667–3689.

[5] R.M. Bruce, J. Santodonato M.W. Neal, Summary review of the health effects associated with phenol, Toxicol. Ind. Health, 3 (1987) 535–568.

[6] World Health Organization, Health Criteria and Supporting Information, WHO Guidelines for Drinking Water Quality (vol. II), Geneva, Switzerland, 1984.

[7] M. Rafatullah, O. Sulaiman, R. Hashim, A. Ahmad, Adsorption of methylene blue on low-cost adsorbents: a review, J. Hazard. Mater., 177 (2010) 70–80.

[8] S. Zhang, J. Li, X. Wang, Y. Huang, M. Zeng, J. Xu, Rationally designed 1D Ag@ $AgVO_3$ nanowire/graphene/protonated gC_3N_4 nanosheet heterojunctions for enhanced photocatalysis via electrostatic self-assembly and photochemical reduction methods, J. Mater. Chem. A, 3 (2015) 10119–10126.

[9] G.E. Box, K.B. Wilson, On the experimental attainment of optimum conditions, Roy. Statist. Soc, Ser. B, 13 (1951) 1–45.

[10] M. Ghaedi, S. Hajati, M. Zare, M. Zare, S.Y. Shajaripour Jaberi, Experimental design for simultaneous analysis of malachite green and methylene blue; derivative spectrophotometry and principal component-artificial neural network, RSC Adv., 5 (2015) 38939–38947.

[11] A. Asfaram, M. Ghaedi, S. Agarwal, I. Tyagi, V.K. Gupta, Removal of basic dye Auramine-O by ZnS: Cu nanoparticles loaded on activated carbon: optimization of parameters using response surface methodology with central composite design, RSC Adv., 5 (2015) 18438–18450.

[12] J.N. Sahu, J. Acharya, B.C. Meikap, Response surface modeling and optimization of chromium (VI) removal from aqueous solution using tamarind wood activated carbon in batch process, J. Hazard. Mater., 172 (2009) 818–825.

[13] Z. Alam, S.A. Muyibi, J. Toramae, Statistical optimization of adsorption processes for removal of 2 4-dichlorophenol by activated carbon derived from oil palm empty fruit bunches, J. Environ. Sci., 19 (2007) 674–677.

[14] P. Ricou-Hoeffer, I. Lecuyer, P.L. Cloirec, Experimental design methodology applied to adsorption of metallic ions onto fly ash, Water Res., 35 (2001) 965–976.

[15] U.K. Garg, M.P. Kaur, V.K. Garg, D. Sud, Removal of nickel (II) from aqueous solution by adsorption on agricultural waste biomass using a response surface methodological approach, Bioresour. Technol., 99 (2008) 1325–1331.

[16] R.M. Aghav, S. Kumar, S.N. Mukherjee, Artificial neural network modeling in competitive adsorption of phenol and resorcinol from water environment using some carbonaceous adsorbents, J. Hazard. Mater., 188 (2011) 67–77.

[17] K. Yetilmezsoy, S. Demirel, Artificial neural network (ANN) approach for modeling of Pb (II) adsorption from aqueous solution by Antep pistachio (Pistacia Vera L.) shells, J. Hazard. Mater., 153 (2008) 1288–1300.

[18] K.V. Kumar, K. Porkodi, R.L. Avila Rondon, F. Rocha, Neural network modeling and simulation of the solid/liquid activated carbon adsorption process, Ind. Eng. Chem. Res., 47 (2008) 486–490.

[19] H.P. Boehm, Some aspects of the surface chemistry of carbon blacks and other carbons, Carbon, 32(1994) 759–769.

[20] B.M. Babić, S.K. Milonjić, M.J. Polovina, B.V. Kaludierović, Point of zero charge and intrinsic equilibrium constants of activated carbon cloth, Carbon, 37 (1999) 477–481.

[21] M. Mastalerz, R.M. Bustin, Application of reflectance micro-Fourier transform infrared spectrometry in studying coal macerals: comparison with other Fourier transform infrared techniques, Fuel, 74 (1995) 536–542.

[22] N. Aktaş, Optimization of biopolymerization rate by response surface methodology (RSM), Enzyme Microb. Technol., 37 (2005) 441–447.

[23] A. Shukla, Y.H. Zhang, P. Dubey, J.L. Margrave, S.S. Shukla, The role of sawdust in the removal of unwanted materials from water, J. Hazard. Mater., 95 (2002) 137–152.

[24] M. Bansal, D. Singh, V.K. Garg, A comparative study for the removal of hexavalent chromium from aqueous solution by agriculture wastes' carbons, J. Hazard. Mater., 171 (2009) 83–92.

[25] W. Daoud, T. Ebadi, A. Fahimifar, Optimization of hexavalent chromium removal from aqueous solution using acid-modified granular activated carbon as adsorbent through response surface methodology, Korean J. Chem. Eng., 32 (2015) 1119–1128.

[26] B. Agarwal, C. Balomajumder, P.K. Thakur, Simultaneous co-adsorptive removal of phenol and cyanide from binary solution using granular activated carbon, Chem. Eng. J., 228 (2013) 655–664.

[27] E.A. Dil, M. Ghaedi, A.M. Ghaedi, A. Asfaram, A. Goudarzi, S. Hajati, M. Soylak, S. Agarwal, V.K. Gupta, Modeling of quaternary dyes adsorption onto ZnO–NR–AC artificial neural network: Analysis by derivative spectrophotometry, J. Ind. Eng. Chem., 34 (2016) 186–197.

[28] B. Hameed, Spent tea leaves: a new non-conventional and low-cost adsorbent for removal of basic dye from aqueous solutions, J. Hazard. Mater., 161 (2009) 753–759.

[29] S. Lagergren, About the theory of so-called adsorption of soluble substances, K. Sven. Vetenskapsakad., Hl., 24 (1898) 1–39.
[30] Y.S. Ho, G. McKay, Pseudo-second order model for sorption processes, Process Biochem., 34 (1999) 451–465.
[31] M. Özacar, İ.A. Şengil, A kinetic study of metal complex dye sorption onto pine sawdust, Process Biochem., 40 (2005) 565–572.
[32] I. Langmuir, Chemical reactions at low pressures, J. Am. Chem. Soc., 37 (1915) 1139–1167.
[33] T.W. Weber, R.K. Chakravorti, Pore and solid diffusion models for fixed bed adsorbers, AIChE Journal, 20 (1974) 228–238.
[34] H.M.F. Freundlich, Over the adsorption in solution, J. Phys. Chem., 57 (1906) 385–470.
[35] G.S. Agarwal, H.K. Bhuptawat Chaudhari, Biosorption of aqueous chromium (VI) by Tamarindus indica seeds, Bioresour. Technol., 97 (2006) 949–956.
[36] J.C. Lazo-Cannata, A. Nieto-Márquez, A. Jacoby, A.L. Paredes-Doig, A. Romero, M.R. Sun-Kou, J.L. Valverde, Adsorption of phenol and nitrophenols by carbon nanospheres: Effect of pH and ionic strength , Sep. Purif. Technol., 80 (2011) 217–224.
[37] A. Gupta, C. Balomajumder, Simultaneous adsorption of Cr(VI) and phenol onto tea waste biomass from binary mixture: multicomponent adsorption, thermodynamic and kinetic study, J. Envir. Chem. Eng., 3 (2015) 785–796.
[38] A. Gupta, C. Balomajumder, Simultaneous removal of Cr(VI) and phenol from binary solution using Bacillus sp. immobilized onto tea waste biomass, J. Water. Process. Eng., 6 (2015) 1–10.